Polyhedron 28 (2009) 883–890

Contents lists available at ScienceDirect

Polyhedron

journal homepage: www.elsevier.com/locate/poly

The pH-specific synthesis, spectroscopic, structural, and magnetic properties of a new Ni(II) species containing the plant physiological binder D-(−)-quinic acid: Association with the aqueous speciation of the binary Ni(II)–quinate system

M. Menelaou [a], C. Mateescu [b], H. Zhao [c], N. Lalioti [d], A. Salifoglou [a,*]

[a] Department of Chemical Engineering, Aristotle University of Thessaloniki, Thessaloniki 54124, Macedonia, Greece
[b] Banat's University of Agricultural Sciences and Veterinary Medicine, Timisoara 300645, Romania
[c] Department of Chemistry, University of Puerto Rico, San Juan, PR 00931-3346, USA
[d] Department of Chemistry, University of Patras, Patras 26500, Greece

ARTICLE INFO

Article history:
Received 19 August 2008
Accepted 24 December 2008
Available online 31 January 2009

Keywords:
Nickel(II)–quinate binary interactions
Aqueous structural speciation
X-ray structure
Solid state-solution structure correlation
Nickel toxicity

ABSTRACT

Nickel is an element present in the abiotic and biological world. In its capacity to promote chemistry at the cellular level, Ni(II) interacts with physiological ligands, thus influencing physiological or pathological conditions. Efforts to comprehend the underlying chemistries led to the investigation of Ni(II) reactivity toward the physiological D-(−)-quinic acid, under pH-specific conditions, facilitating the isolation of a new species $Na[Ni(C_7H_{11}O_6)_3] \cdot 2.75H_2O$ (**1**). Compound **1** was characterized by elemental analysis, spectroscopic techniques (FT-IR, UV–Visible), magnetic susceptibility studies, and X-ray crystallography. The lattice of **1** reveals the presence of an octahedral Ni(II) complex bound to three quinate ligands through the α-hydroxycarboxylate group, thus projecting a stable entity. Concurrent aqueous speciation studies on the Ni(II)–quinate binary system unravel the nature and properties of species arising from Ni(II)–quinate interactions. To this end, the structural and spectroscopic properties of **1**, in the solid state and in solution, are in line with the aqueous speciation, exemplifying key features of Ni(II) interactions with the low molecular mass quinic acid in biologically relevant fluids. The overall physicochemical profile of **1** projects well-defined soluble and potentially bioavailable Ni(II) species that could be involved in specific chemical processes and (bio)chemical reactivity patterns at the physiological or molecular toxicity level.

1. Introduction

Nickel has since long been recognized as a chemical element present in the earth's crust and in the bacterial, fungal and plant world [1]. In the abiotic world, nickel is a metal used to produce stainless steel and other metal alloys [2] for making coins, jewelry, and items such as valves and heat exchangers [3]. Concurrently, many studies have been carried out to investigate proteins and enzymes that bind nickel. These diverse biological systems participate in nickel acquisition, transport and storage, regulation and maturation of nickel metalloenzymes, etc. [4]. To that end, nickel, as a metal cofactor, plays an important role in metalloenzymes such as carbon monoxide dehydrogenase (CODH), methyl-CoM reductase, acetyl-CoA synthase (ACS), Ni–Fe hydrogenases, urease, Ni-superoxide dismutase, and glyoxalase I [5].

Metal ions in all biological systems are mobilized efficiently through interactions with organic substrates–ligands capable of coordinating them and solubilizing them in cellular fluids. These ligands include both low and high molecular mass binders. Ni(II) can coordinate such ligands and promote further ternary interactions with other biological targets. The chemistry of those aqueous interactions is closely linked with any physiological or toxic manifestations that this metal ion can bring about. One such metal ion binder is the low molecular mass molecule D-(−)-quinic acid, 1α,3α,4α,5β-tetrahydroxy-1-cyclohexane carboxylic acid. It is found widely in plants. There, it is encountered as a precursor to shikimic acid, [6,7] which is involved in the biosynthesis of aromatic amino acids. In this sense, quinic acid rises as a vital molecule in cellular physiology [8]. Metal ions, such as Mn(II), Zn(II), and Cu(II), can coordinate to polyfunctional quinic acid, a chelator bearing three very important features: (a) a carboxylate moiety known to promote metal ion binding, (b) an alcoholic moiety α- to the carboxylate group, and (c) three alcoholic groups relevant to polyol functionalities. Hence, coordination of quinic acid to metal ions, such as Ni(II), is expected to promote solubilization and lead to metallo(bio)chemical interactions shedding light onto the role of that metal ion in cellular fluids not unlike that of a plant.

On the basis of the above views, the paucity of low molecular mass Ni(II)–quinate soluble forms leads to the exploration of the

* Corresponding author. Tel.: +30 2310 996 179; fax: +30 2310 996 196.
E-mail address: salif@auth.gr (A. Salifoglou).

0277-5387/$ - see front matter © 2009 Elsevier Ltd. All rights reserved.
doi:10.1016/j.poly.2008.12.045

aqueous interactions and ensuing chemistry of Ni(II) with the α-hydroxycarboxylate binder D-(−)-quinic acid. This chemistry is expected to (a) enlighten the type and nature of interactions emerging into the structural speciation of the requisite binary Ni(II)–hydroxycarboxylate cellular systems, and (b) provide insight into the chemical and physical properties on new Ni(II) species emerging as potential metallo(bio)targets in cellular physiology or toxicity. To this end, we, herein, report on the pH-specific synthesis, spectroscopic and structural characterization, and magnetic susceptibility studies of a new binary Ni(II)–quinate species $Na[Ni(C_7H_{11}O_6)_3] \cdot 2.75H_2O$ **(1)** closely tied to the aqueous speciation of the binary system and its significance in Ni(II) biologically relevant chemistry.

2. Experimental

2.1. Materials and methods

All manipulations were carried out under aerobic conditions. $NiCl_2 \cdot 6H_2O$ and D-(−)-quinic acid (purity 98%) were purchased from Fluka. Nano-pure quality water was used for all reactions run. NaOH and NaCl were supplied by Fluka.

2.2. Physical measurements

FT-IR measurements were taken on a 1760X FT-IR spectrometer from Perkin–Elmer, using KBr pellets. UV–Visible measurements were carried out on a Hitachi U2001 spectrophotometer in the range from 190 to 1000 nm. A ThermoFinnigan Flash EA 1112 CHNS elemental analyzer was used for the simultaneous determination of carbon and hydrogen (%). The analyzer is based on the dynamic flash combustion of the sample (at 1800 °C) followed by reduction, trapping, complete GC separation and detection of the products. The instrument is (a) fully automated and controlled by PC via the Eager 300 dedicated software and (b) capable of handling solid, liquid or gaseous substances. Magnetic susceptibility data were collected on powdered samples of **1** with a Quantum Design SQUID susceptometer in the 2–300 K temperature range, under various applied magnetic fields. Magnetization measurements were carried out at three different temperatures in the field range 0–5 T.

2.3. pH-potentiometric measurements

The protonation constants of quinic acid were determined by pH-potentiometric titrations of 30.0(1) ml samples in the pH range 2.8–11.4 under a purified argon atmosphere. The concentration of quinic acid was in the range of 1.3–5.0 mmol dm^{-3}. The stability constants of the Ni(II) complexes of quinic acid were determined by pH-potentiometric titrations of 30.0(1) ml samples in the pH range 2.4–8.7 under a purified argon atmosphere. Precipitation was observed at pH ~8.7, as in the case of the aqueous binary system of Co(II) with 2′-deoxyguanosine 5′-monophosphate [9].

All solutions were prepared using Fluka reagent grade quinic acid, $NiCl_2 \cdot 6H_2O$, and ultra-pure deionized water. The purity of quinic acid and the exact concentration of quinate and Ni(II) solutions, were determined by the Gran method [10–12]. The exact concentration of Ni(II) was checked by EDTA complexometric titrations as previously described [13]. The ionic strength was adjusted to 0.15 M with NaCl. The temperature was maintained at 25.0 ± 0.1 °C during the measurements. The titrations were carried out with a carbonate-free NaOH solution of known concentration (ca. 0.15 M). The base solution was prepared following a standard procedure: NaOH pellets were dissolved in nano-pure quality water under an argon atmosphere. Carbon dioxide was removed from water by boiling and cooling under a stream of purified argon. The NaOH solution was standardized using potassium hydrogen iodate ($KH(IO_3)_2$). The nickel concentration was 1.0 mM, and the employed metal:ligand ratios were 1:2, 1:3, and 1:4. In order to collect solution data at pH values lower than 3.0, a known amount of nitric acid was initially added. The pH was measured with a computer-controlled Crison titration system elaborated for titrations at such low concentrations [14] and a Mettler Toledo-Inlab 412 combined glass-electrode, calibrated for hydrogen ion concentration according to Irving et al. [15] by using the GLEE program [16]. The ionic product of water was found to be $pK_w = 13.76$ [17].

The one step protonation constants of quinic acid are given as $\log K_1$, consistent with the equilibrium $L^- + H^+ \rightleftarrows HL$, where $K_1 = [HL]/[L^-] \rightleftarrows [H^+]$. The stepwise protonation constants of quinic acid are given as $\log K_n$, consistent with the equilibrium $H_{n-1}L + H \rightleftarrows H_nL$, where $K_n = [H_nL]/[H_{n-1}L]\,[H]$. The initial computations were obtained in the form of overall protonation constants $\beta_n = [H_nL]/[L]\,[H]^n$, taking into account that $\beta_n = \prod K_n$. The concentration stability constants $\beta_{pqr} = [M_pL_qH_r]/[M]^p[L]^q[H]^r$ for quinic acid were calculated with SUPERQUAD [18], and those for Ni(II)–quinate complexes, arising in the investigated system, with the PSEQUAD computer program [19]. The pH-dependent species distribution curves and simulated titration curves were derived from the overall formation constants measured with the program HYSS [20].

Formation of Ni(II)–hydroxo complexes was taken into consideration in the employed calculations leading to the most plausible speciation model. The hydroxo species considered include the following: (a) $[NiH_{-1}]^+$ ($\log\beta_{1-1} = -9.74$), (b) $[Ni_2H_{-1}]^{3+}$ ($\log\beta_{2-1} = -9.6$), and (c) $[Ni_4(OH)_4]^{4+}$ ($\log\beta_{4-4} = -27.4$). Relevant information on the above species was taken from Plyasunova et al. [21] and corrected for an ionic strength of 0.15 M by use of the Davies equation [22].

2.4. Synthesis of sodium [tris(quinato)nickel(II)] hydrate: $Na[Ni(C_7H_{11}O_6)_3] \cdot 2.75H_2O$ (**1**)

$NiCl_2 \cdot 4H_2O$ (0.50 g, 2.1 mmol) and D-(−)-quinic acid (0.80 g, 4.2 mmol) were placed in a 25 mL round bottom flask and dissolved in 6 mL of water. The reaction mixture was then stirred at room temperature until both reactants were completely dissolved. Subsequently, the pH of the clear solution was adjusted to 5.5 with NaOH. The resulting reaction mixture was placed in the refrigerator at 4 °C and ethanol was added. Four months later, green crystalline material appeared on the bottom of the flask. The crystalline product was isolated by filtration and dried in vacuo. Yield 0.62 g (36%). *Anal.* Calc. for **1**, $Na[Ni(C_7H_{11}O_6)_3] \cdot 2.75H_2O$ ($C_{21}H_{38.50}O_{20.75}NaNi$, MW = 704.47): C, 35.7; H, 5.5. Found: C, 35.0; H, 5.8%.

2.5. X-ray crystal structure determination

X-ray quality crystals of compound **1** were grown from reaction mixtures upon addition of ethanol. A single crystal with dimensions 0.50 × 0.30 × 0.20 mm (**1**) was mounted on the tip of a glass fiber with epoxy glue. Single crystal analysis was carried out on a Bruker AXS SMART 1K CCD area detector diffractometer. The frame data were acquired at room temperature using the SMART-NT software and Mo Kα radiation ($\lambda = 0.71073$ Å) [23]. A total of 1325 45-s frames were collected in three sets with 0.3° ω-scan. The collected frames were then processed using the SAINT-NT software [24] to provide the *hkl* file corrected for Lorentz and polarization effects. An empirical absorption correction was applied through the program SADABS [23]. The structure was solved by direct methods using the SHELX-90 program and refined by least-squares methods on F^2, SHELXTL-93, incorporated in SHELXTL, Version 5.1 (Table 1) [25].

Table 1
Summary of crystal, intensity collection and refinement data for Na[Ni-($C_7H_{11}O_6$)$_3$] · 2.75H_2O (1).

Formula	$C_{21}H_{38.50}O_{20.75}NaNi$
Formula weight	704.47
T (K)	293(2)
Wavelength	Mo Kα 0.71073
Space group	$P2_12_12_1$
a (Å)	15.330(3)
b (Å)	15.453(3)
c (Å)	16.660(3)
β (°)	90.00
V (Å^3)	3946.9(11)
Z	4
D_{calc}/D_{measd} (Mg m^{-3})	1.186/1.89
Absorbtion coefficient (μ) mm^{-1}	0.570
Range of h, k, l	−18 → 18, −17 → 19, −12 → 20
Goodness-of-fit on F^2	1.147
R indices[a]	R = 0.0653, R_w = 0.2038[b]

[a] R values are based on F values, R_w values are based on F^2. $R = \frac{\sum||F_0|-F_c||}{\sum(|F_0|)}$, $R_w = \sqrt{\sum[w(F_0^2 - F_c^2)^2]/\sum[w(F_0^2)^2]}$.

[b] For 7735 reflections with $I > 2\sigma(I)$.

All non-hydrogen atoms were refined anisotropically. Hydrogen atoms on carbon atoms were geometrically positioned and left riding on their parent atoms during structure refinement. Hydrogen atom positions, which belong to oxygen atoms, were first determined from E-maps, brought to reasonable distances from their parent oxygen atoms, and then fixed. The disordered oxygen-atoms of water were left as such (nascent form). The final assignment of hydrogen atoms satisfies the electroneutrality of compound **1**, with the understanding that Ni ions are formally in the +2 oxidation state. The associated CCDC reference number is 644650. Selected crystallographic data appear in Table 1. Further crystallographic details for **1**: $2\theta_{max}$ = 52°; reflections collected/unique/used, 23772/7735 [R_{int} = 0.0471]; 415 parameters refined; $[\Delta\rho]_{max}/[\Delta\rho]_{min}$ = 0.917/−0.399 e/Å^3; R/R_w (for all data), 0.0841/0.2127.

3. Results

3.1. Synthesis

Complex **1** was synthesized through a simple reaction between Ni(II) and D-(−)-quinic acid in a 1:2 molar ratio and isolated by addition of ethanol to the reaction mixture. The presence of NaOH helped to adjust the pH of the reaction mixture, while concurrently providing the appropriate counter ions to balance the arisen charge on the Ni(II)–quinate assembly (vide infra). The same reaction run with a Ni(II):quinic acid a 1:3 molar ratio led to a material identical to **1** by virtue of its FT-IR signature (yield 33%). A major advantage, however, of this reaction was that the crystalline product was obtained faster than that of the 1:2 Ni(II):quinic acid ratio. The stoichiometric reaction leading to the formation of compound **1** is shown below (Reaction 1):

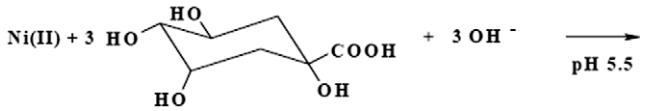

D-(-)-quinic acid

$[Ni(C_7H_{11}O_6)_3]^-$ + 3 H_2O Reaction 1

Elemental analysis of the isolated green-colored crystalline material and FT-IR spectroscopy suggested the molecular formula Na[Ni-($C_7H_{11}O_6$)$_3$] · 2.75H_2O for **1**. Confirmation came from the X-ray crystallographic determination of its structure. Compound **1** is soluble in water, but insoluble in common organic solvents. Crystalline **1** is stable in the air at room temperature for long periods of time.

3.2. Description of X-ray crystallographic structure

Compound **1** emerges from a crystal lattice composed of discrete anionic Ni(II) complexes and Na^+ counter ions. The structure diagram for complex **1** is shown in Fig. 1. A list of selected bond distances and angles for **1** is given in Table 2. Complex **1** crystallizes in the orthorhombic space group $P2_12_12_1$ with four molecules per unit cell. The X-ray crystal structure of **1** reveals a Ni(II) assembly, with three quinate ligands coordinating to the metal ion through the alcoholic and carboxylate oxygens O(1) and O(5), O7 and O11, and O13 and O17, respectively. Each bound ligand is singly deprotonated, with the site of deprotonation being the carboxylic acid group. The three bound quinates formulate a distorted octahedral environment around Ni(II). Unlike other metal ions (e.g. Mn(II)) bound to the quinate ligand, the Ni(II) ion bears quinate ligands, the terminal alcoholic moieties of which do not participate in coordination to abutting metal ions in the crystal lattice of the title compound lattice.

The Ni–O bond distances are in the range from 2.009(4) to 2.069(4) Å for **1**, which are comparable with those in complexes, $(NH_4)_2[Ni_2(C_6H_5O_7)_2(H_2O)_4]_2 \cdot 2H_2O$ (2.020(3)–2.074(2) Å) (**2**) [26], $K_2[Ni(C_6H_5O_7)_2(H_2O)_4] \cdot 4H_2O$ (2.036(3)–2.125(3) Å) (**3**) [27], $[Ni(C_4H_4O_5)(H_2O)] \cdot H_2O$ (2.034(5)–2.101(5) Å) (**4**), $[Ni(C_4H_4O_5)(H_2O)(C_{12}H_8N_2)]$ (2.032(3)–2.048(3) Å) (**5**) [28], and $[(N(CH_3)_4)_5[Ni_4(C_6H_4O_7)_3(OH)(H_2O)] \cdot 18H_2O]_2$ (1.95(1)–2.12(1) Å) (**6**) [29].

The angles are in the range 77.99(15)–102.76(19)° for complex **1** and similar to those observed in (81.53(9)–96.7(2)°) (**2**), (86.8(1)–95.2(1)°) (**3**), (81.1(2)–95.0(2)°) (**4**), (89.2(2)–95.1(2)°) (**5**), (76.5(4)–102.1(4)°) (**6**), and also similar to those in the quinate organic–inorganic hybrid $[Mn_2(C_7H_{11}O_6)_4]_n \cdot nH_2O$ (69.56(15)–96.75(17)° and 73.02(13)–95.41(15)°, respectively) [30].

The octahedral Ni(II) ion in **1** correlates well with other octahedral divalent metal ions such as Zn(II) [31], Cu(II) [32], and Ni(II) [25], in analogous octahedral species bearing citrates. The M–O distances observed in those complexes are in line with those seen

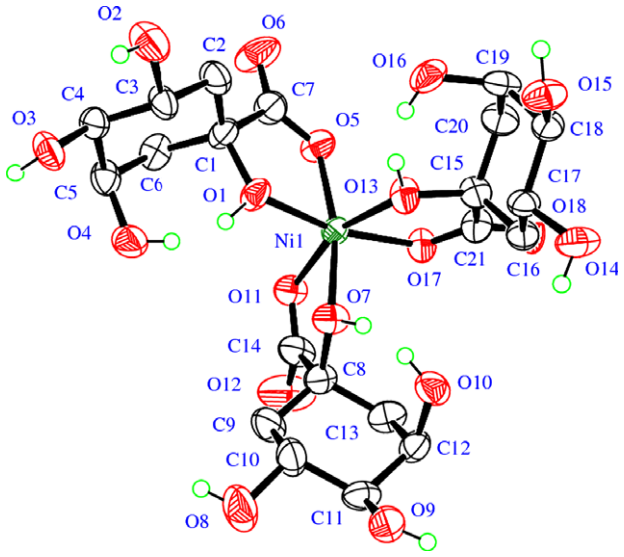

Fig. 1. The structure of the anionic assembly in Na[Ni($C_7H_{11}O_6$)$_3$]·2.75H_2O (**1**) with the atom-labeling scheme (50% thermal probability ellipsoids).

Table 2
Bond lengths (Å) and angles (°) in **1**.

Distances			
Ni(1)–O(1)	2.039(4)	Ni(1)–O(11)	2.041(4)
Ni(1)–O(5)	2.009(4)	Ni(1)–O(13)	2.069(4)
Ni(1)–O(7)	2.031(4)	Ni(1)–O(17)	2.005(4)
Angles			
O(17)–Ni(1)–O(5)	94.62(18)	O(7)–Ni(1)–O(11)	79.58(17)
O(17)–Ni(1)–O(7)	98.70(19)	O(1)–Ni(1)–O(11)	102.76(19)
O(5)–Ni(1)–O(7)	166.49(18)	O(17)–Ni(1)–O(13)	77.99(15)
O(17)–Ni(1)–O(1)	165.95(18)	O(5)–Ni(1)–O(13)	98.3(2)
O(5)–Ni(1)–O(1)	79.16(16)	O(7)–Ni(1)–O(13)	86.78(18)
O(7)–Ni(1)–O(1)	88.32(17)	O(1)–Ni(1)–O(13)	90.36(17)
O(17)–Ni(1)–O(11)	90.52(17)	O(11)–Ni(1)–O(13)	160.67(17)
O(5)–Ni(1)–O(11)	98.10(19)		

in **1** and range from 2.052(2) to 2.164(2) Å (Zn(II)) and from 2.021(3) to 2.072(3) Å (Ni(II)), while a wider range due to Jahn–Teller distortion is observed in the copper analog (1.969(3)–2.341(3) Å). Equally comparable are the M–O distances with those occurring in the congener quinate compounds $[Zn(C_7H_{11}O_6)_2]$ [33], $[Cd(C_7H_{11}O_6)_2]\cdot H_2O$, $[Cu(C_7H_{10}O_6)(H_2O)]_2(H_2O)_2$ [34], $\{[Cu(NO_3)(C_7H_{11}O_6)(H_2O)]\cdot 2H_2O\}_n$, $\{[CuCl(C_7H_{11}O_6)(H_2O)]\cdot H_2O\}_n$ [35], $[Pt(C_6H_{14}N_2)(C_7H_{10}O_6)]$ [36], and the trinuclear $(NH_4)_2\{[V(O)_2]_2[V(O)](\mu\text{-}C_7H_{10}O_6)_2\}\cdot H_2O$ [37].

In the lattice structure, the Na^+ ions counterbalance efficiently the anionic charge. They are in contact with the alcoholic oxygens of the quinate anion at distances in the range of 2.344(6)–2.423(5) Å (six contacts) (Fig. 2B). The crystal structure of **1** is composed of an infinite 3D network, where quinate ligands bridge each Ni-atom with its three neighboring Na-atoms. The three Na-atoms define a triangle, with the Ni-atom located above its center and the Ni–Na distance in the range 8.083(3)–8.096(3) Å (Fig. 2A). Each Na^+ ion is bound to three quinates, all originating from different $[Ni(C_7H_{11}O_6)_3]^-$ units.

3.3. UV–Visible spectroscopy

The UV–Visible spectrum of **1** was recorded in water (Fig. S1). The spectrum exhibits peaks at λ_{max} 725 (ε 2 M^{-1} cm^{-1}) and 662 nm (ε 2 M^{-1} cm^{-1}), and a distant shoulder around 395 nm rising into the UV. The absorption feature around 395 nm (ε 6 M^{-1} cm^{-1}) could be tentatively attributed to the $^3A_{2g} \rightarrow {}^3T_{1g}(P)$ transition. The observed multiple structure containing the 725 and 662 nm features, a region normally corresponding to the $^3A_{2g} \rightarrow {}^3T_{2g}$ transition, is in line with literature reports invoking the presence of an ^1E_g state lying so close to $^3T_{2g}$ that extensive mixing takes place. That mixing leads to the observation of a doublet band, where the spin forbidden transition picks up intensity from the spin-allowed transition, thus accounting for the complexity of the spectrum [38]. The spectrum bears similar features to that of $[Ni(H_2O)_6]^{2+}$ ion, signifying the effect of the O-containing ligands in the electronic structure of Ni(II).

3.4. FT-IR spectroscopy

The FT-IR spectrum of **1** exhibits strong absorptions for the carbonyls of the carboxylate groups in both the antisymmetric and symmetric vibration regions. The antisymmetric stretching vibrations $\nu_{as}(COO^-)$ appear close to 1602 cm^{-1}, whereas the symmetric stretches $\nu_s(COO^-)$ appear in the range 1450–1334 cm^{-1}. The frequencies for the carbonyl stretches in **1** are shifted to lower values compared to those of the free quinic acid. In addition to this, they indicate a change in the vibrational status of the quinate anion upon coordination to the metal ion. The difference between the symmetric and antisymmetric stretches, $\Delta(\nu_{as}(COO^-) - \nu_s(COO^-))$, was greater than 200 cm^{-1}, indicating that the carboxylate groups of the quinate ligand were either free or coordinated to the metal ion in a monodentate fashion [39,40]. The latter contention was further confirmed by the X-ray crystal structure of **1**. Similar trends in the frequencies of the carboxylate carbonyls have also been observed in the FT-IR spectra of other metal–quinate complexes as well as α-hydroxycarboxylate complexes with metal ions [41,42].

3.5. Magnetic susceptibility studies

Magnetic susceptibility measurements were carried out at different magnetic fields and in the temperature range 2–300 K. The data were fitted with the MAGPACK [43] program, employed with a nonlinear least-squares curve-fitting program, DSTEPIT [44]. The temperature dependence of $\chi_M T$ (χ_M being the magnetic suscepti-

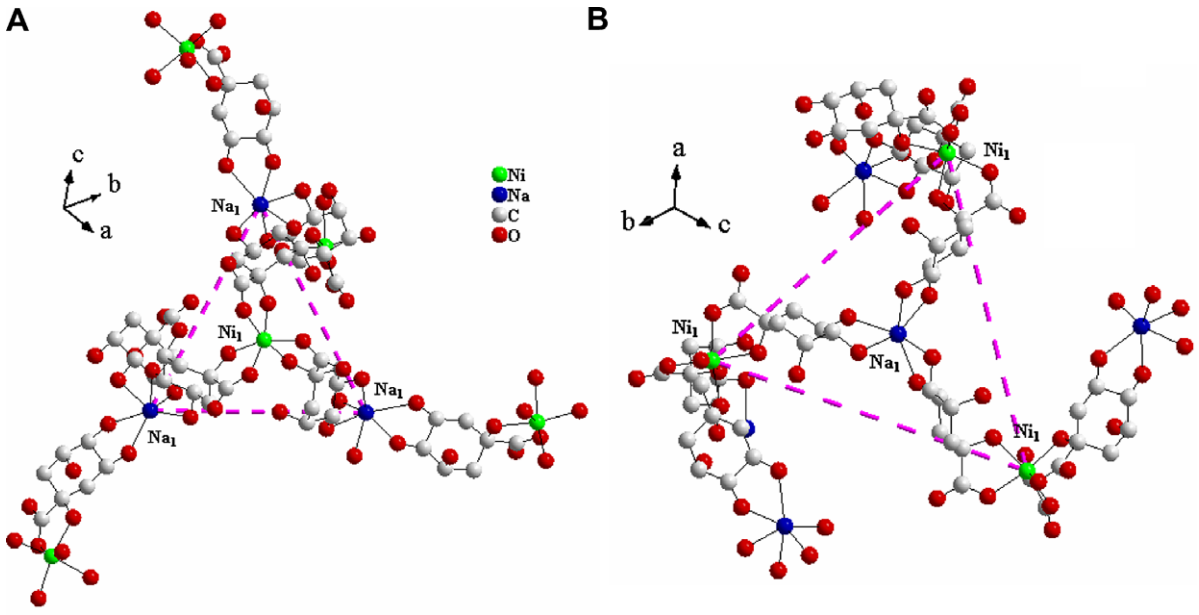

Fig. 2. Structural organization of **1**, showing the relationship between Na- and Ni-atoms (A and B) in the lattice composition (see text).

bility for one Ni(II) ion) for complex **1** is shown in Fig. 3 (solid circles). The $\chi_M T$ value is 1.78 emu mol^{-1} K at 300 K. From that temperature down to 10 K there is a smooth linear decrease, while after that temperature and until 2 K a more pronounced decrease occurs, reaching the value of 0.84 emu mol^{-1} K. The shape of this curve is characteristic of the occurrence of large zero field effects along with the temperature independent paramagnetism effect, TIP, which leads to a linear temperature dependence of the susceptibility data. The susceptibility data were fitted by the following equation:

$$H = D\left[S_z^2 - \frac{1}{3}S(S+1)\right] + E(S_x^2 - S_y^2) + g_z\mu_B H_z S_z + g_x\mu_B H_x S_x + g_y\mu_B H_y S_y, \quad (1)$$

where an isotropic g-value was used. The best fit (solid line in Fig. 3) is given by the parameters $D = 3.4$ cm^{-1} and $g = 2.2$, TIP = 1.8×10^{-3}. In the inset of the figure, simulations of the susceptibility function are shown for different values of the D parameter, where the g value and the TIP were kept at values obtained from the fitting procedure. Both axes are in logarithmic scale.

Isothermal magnetization curves at T 2 K in the applied field 0–5 T are shown in Fig. 4. The curves for the increasing and decreasing fields are identical. The data were fitted using (Eq. (1)) and the best fit (solid line in Fig. 4) is given by the parameters of $D = 2.8$ cm^{-1}, $g = 2.2$. The latter are very close to the values obtained from the susceptibility study, verifying the large zero-field character of the system.

3.6. Speciation studies

pH-potentiometric titrations of the ligand quinic acid alone, and Ni(II) with D-(−)-quinic acid in various metal ion to ligand molar ratios [Ni:L] = [1:2/1:3/1:4] were carried out. The titration curves were evaluated with different potential speciation models. The best fit between the experimental and calculated titration curves for the binary Ni(II)–quinic acid system was obtained by considering the species [Ni(II)], $[NiL_2]^o$ (HL = $C_7H_{12}O_6$; L = $C_7H_{11}O_6^-$), $[NiL_2H_{-1}]^-$, and $[NiH_{-1}]^+$. The fit is reasonably good in the overall pH and concentration range used, demonstrating that the adopted speciation model is satisfactorily defined. Other complexes, such as 1:1 and 1:2 Ni(II):quinate complexes or variably protonated and deprotonated species were rejected by the computer program (PSEQUAD) during the computation process. The species emerging from the speciation distribution of the binary system are in good agreement with the corresponding species synthesized and isolated in the solid state. The stability constants of the complexes formed are listed in Table 3. The uncertainties (3SD values) for the stability constants are given in parentheses. The pH range of the optimal formation of complexes is also reported. For the titratable quinate carboxylate group, the pK_a value of 3.34 was obtained and was found to be very close to the values reported by Clifford (3.40) [45] and Luethy-Krause et al. (3.36) [46]. For shikimic acid (3R, 4S, 5R)-3,4,5-trihydroxy 1-cyclohexanecarboxylic acid) the pK_a value is 4.15 [45]. The presence of an alcoholic moiety in a position α- to the carboxylate group of quinic acid increases its acid strength.

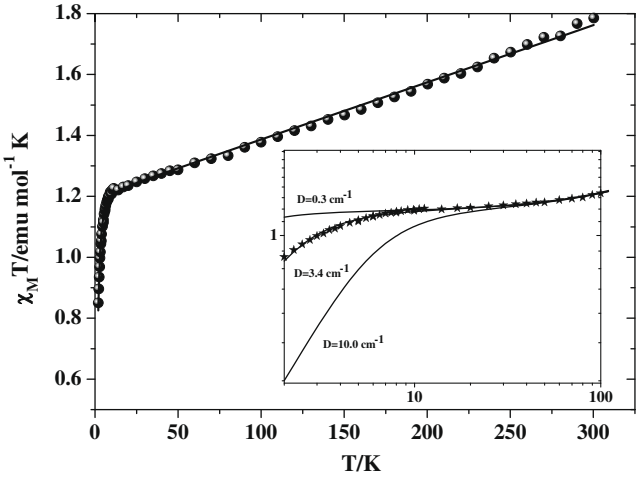

Fig. 3. Temperature dependence of the susceptibility data in the form of $\chi_M T$ vs. T (solid stars) and the fitting results using the theoretical formula discussed in the text (solid line). In the inset, simulations of the susceptibility function are shown, in the form of $\chi_M T$ vs. T, for different values of the D parameter. Both axes are in logarithmic scale.

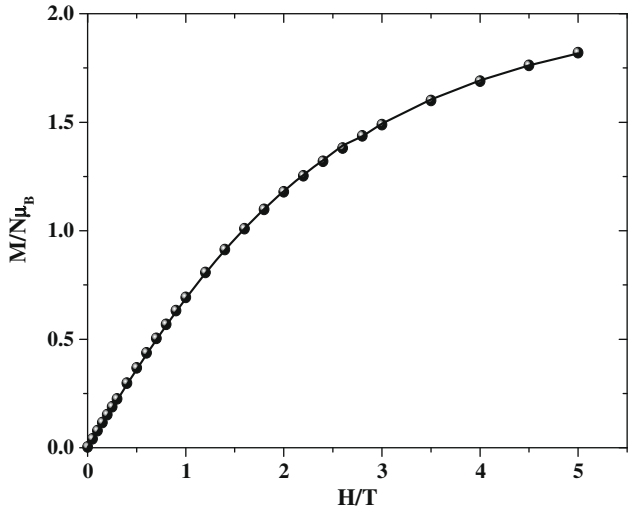

Fig. 4. Magnetization measurements in the field range 0–5 T, at temperature T 2 K, and the fitting results using the theoretical formula discussed in the text (solid line).

The titrimetric data were evaluated on the premise that complex formation between Ni(II) and quinate proceeds through binding of the quinate carboxylate and the α-alcoholic group moieties. The titration curves in the absence and presence of Ni(II) suggest formation of the $[NiL_2]^o$ species in the acidic region up to pH 8, and the $[NiL_2H_{-1}]^-$ species at pH values beyond 7. These studies also suggest that this ligand reacts expediently with Ni(II) ions, forming soluble metal chelate complexes. In the $[NiL_2]^o$ complex, the ligand appears to be deprotonated at the carboxylate moiety and as such both quinate ligands act in a bidentate fashion, coordinating Ni(II). The hexacoordination of Ni(II) ion is consistent with the presence of the $[Ni(H_2O)_6]^{2+}$ complex ion in the entire pH range investigated.

Table 3
Proton (log$K$) and Ni(II)–quinic acid complex formation constants (logβ) at $I = 0.15$ (NaCl) and 25 °C.

	Quinic acid	Ni–quinic acid	pH range for each species
Log$K$(HL)	3.34(1)		
Logβ (NiL_2)		4.95(3)	all domain
Logβ (NiL_2H_{-1})		−4.14(7)	>7.0
pK ($[NiL_2H_{-1}]/[NiL_2]$)		9.09	
Fitting[a]		9.656×10^{-3}	
Number of pts.		191	

Charges from the various species are omitted for clarity.
[a] Goodness-of-fit between the experimental and the calculated titration curves expressed in milliliters of titrant.

The overall stability constant of the mononuclear complex $[NiL_2]^o$ ($\log\beta$ 4.95) is similar yet greater than those in complexes of Ni(II) with some α-hydroxycarboxylic acids, such as 2-hydroxyacetic acid (glycolic acid) ($\log\beta$ 3.77) [47], 2-hydroxypropanoic acid (lactic acid) ($\log\beta$ 2.85) [48], 2-hydroxybutanoic acid ($\log\beta$ 2.89) [49], 2-hydroxy-2-methylpropanoic acid (2-hydroxyisobutyric acid) ($\log\beta$ 2.80) [50], and 2-hydroxy-2-phenylacetic acid (mandelic acid) ($\log\beta$ 2.48) [51].

In the pH range beyond 7 of the binary Ni(II)–quinic acid system, two species emerge, namely $[NiL_2H_{-1}]^-$ and the mononuclear $[NiH_{-1}]^+ = [Ni(OH)]^+$. Quinic acid contains one carboxylic acid group and four alcoholic hydrogens. The pK_a of the latter is >11. The dicationic metal ions (Co(II), Ni(II), etc.) are not sufficiently strong to deprotonate the alcoholic proton of quinic acid. As a consequence, it is very likely that one of the two water molecules coordinated to the nickel ion in the mononuclear species $[NiL_2H_{-1}]^-$ is possibly deprotonated. This is the species arising as the successor participant to the $[NiL_2]^o$ species at higher pH values in the speciation diagram. These two species coexist with the hexa-aquo nickel $[Ni(H_2O)_6]^{2+}$ species in the entire pH range studied, as that is shown in the speciation curves presented in Fig. 5. The maximum% content of $[NiL_2]^o$ appears to be 30% and stays constant in the pH range 4.5–7.5 of the binary Ni(II)–quinic acid system, where $c_{Ni} = 0.000657$ mol dm^{-3}, and $c_{ligand} = 0.002704$ mol dm^{-3}.

Beyond the pH range 8.2–8.8, depending on the molar ratio Ni(II):quinate, a precipitate appears and the pH rise ceases, most likely due to OH^- ions being consumed toward formation of $Ni(OH)_2$. The incipient precipitation at pH beyond 8.5 makes the observation of the next phase of the aqueous speciation doubtful, even in the presence of higher ligand-to-metal molar ratios (Fig. S2).

The presence of the hexa-aquo $[Ni(H_2O)_6]^{2+}$ species over the entire pH range, where the aqueous speciation was investigated, has been noted. In a similar system containing histidinehydroxamic acid, the Ni(II) ion is strongly bound to the ligand in mononuclear NiL ($\log\beta = 10.49$) and NiL_2 ($\log\beta = 18.80$) complexes [52]. From the speciation curves of that system, it can be seen that the hexa-aquo $[Ni(H_2O)_6]^{2+}$ species stays intact up to pH around 11. As was the case of the binary system of Ni(II) in presence of quinic acid, a precipitate appears beyond pH 9 in this system as well. In the Ni(II)–D-glucosamine system [53], the NiL_2 ($\log\beta = 6.43$) complex appears in the pH range 7–10. From the speciation curves of this system, it can be seen that the aquo $[Ni(H_2O)_6]^{2+}$ species stays as such up to pH around 11. Hexa-aquo Ni(II) ions are also the major species present in the binary system of Ni(II) with pycdpnen (a pyridylamido hexadentate ligand) up to pH 7 [54]. In the case of the aqueous binary system of Ni(II) with 2-(4-methylthiazol-2-yl)-2-(hydroxyimino)acetic acid, the binary NiL_2 complex also forms ($\log\beta = 11.83$), while at pH<6.5 hexa-aquo Ni(II) ions are present [55]. The stability constant of the $[NiL_2H_{-1}]^-$ ($\log\beta = -4.14$) species is higher than that of the monohydroxo species $[NiH_{-1}]^+$ ($\log\beta = -9.74$). That could help explain why at pH beyond 7, where both species form, the% content of the $[NiL_2H_{-1}]^-$ species appears to be higher than that of the $[NiH_{-1}]^+$ species in the same pH range [56].

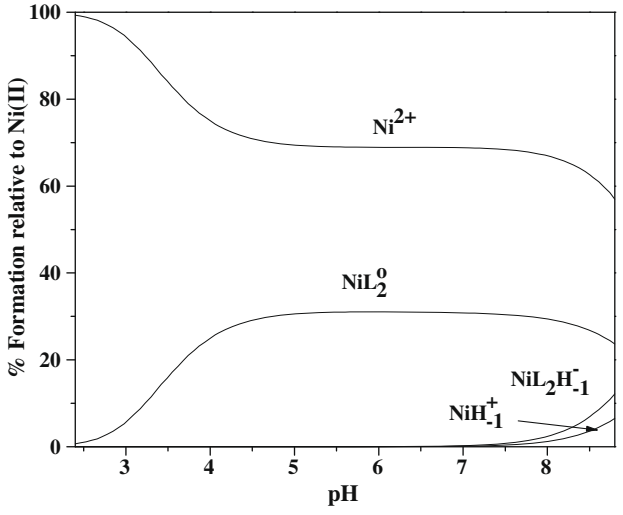

Fig. 5. Speciation curves for complexes forming in the binary Ni(II)–quinic acid system; $c_{Ni} = 0.000657$ mol dm^{-3}, $c_{ligand} = 0.002704$ mol dm^{-3}. Charges are omitted for clarity.

4. Discussion

4.1. The chemistry of the binary Ni(II)–quinate system in aqueous media

The synthesis of $Na[Ni(C_7H_{11}O_6)_3] \cdot 2.75H_2O$ (**1**) through the pH specific reaction of $NiCl_2$ with quinic acid at pH 5.5, emphasizes the distinct interaction of D-(−)-quinic acid with the divalent metal ion Ni(II). The analytical, spectroscopic, structural and magnetic susceptibility characterization of the derived material provided the physical and chemical properties of **1**, revealing a considerable number of structural details related to the reactivity of quinic acid toward Ni(II).

Associated with the distinct structural identity of **1** was the retention of the protonation of the α-alcoholic group in the quinate ligand upon binding to Ni(II). Each binding site around Ni(II) includes the oxygen from the carboxylate moiety bearing 1− charge, thus raising the total charge for the isolated mononuclear complex to 1−. Formation of a five-membered cyclic ring is most likely a source for stability in the isolated complex. The negative charge on the anionic complex $[Ni(C_7H_{11}O_6)_3]^-$ is counteracted by one sodium ion. Retention of the proton of the alcoholic group in the α-position to the carboxylate group has also been observed in the case of the congener α-hydroxycarboxylic acid, citric acid, upon binding of the latter to Ni(II) and Mn(II). In contrast to that behavior, binding of the α-hydroxycarboxylate ligand citrate to the higher oxidation state manganese ion Mn(III), led to a species in which the alcoholic group does not retain the proton despite the fact that citrate employs the same mode of coordination to Mn(III) as in Ni(II), through formation of a five-member cyclic ring [25,57].

Beyond the conventional contributions of the ligand to the reactivity of Ni(II), there appear to be general features potentially involved in the binary Ni(II)–quinic acid system linked to its aqueous chemistry. These include: (a) the coordination mode of all three quinate ligands to Ni(II) in **1**, and (b) the presence of the uncoordinated polyol functionalities in the quinates, signifying the unique chemical reactivity of Ni(II) ions toward α-hydroxycarboxylate ligands (central carboxylate and alcoholic groups) leading to a metal-cyclic motif formation. Even though both the α-hydroxycarboxylate and polyol functionalities in quinate are capable of promoting metal ion binding chemistries, the herein distinctly observed chemical reactivity and structural identity may indicate commensurably diverse chemical reactivity at the biological level. In such an environment, the natural metal ionic binder organic moieties are key molecular targets participating in essential biosynthetic pathways and likely influencing cellular integrity and survival.

Lastly, the employed synthetic strategy for the isolation of complex **1** reflects a chemical reactivity of Ni(II), because of which the title species crystallized out of solution. Key to the achievement of the solid state lattice of **1** appears to be (a) the low solubility of the anionic assembly $[Ni(C_7H_{11}O_6)_3]^-$ in the presence of the counter

ion Na^+, and (b) the involvement of water molecules in the assembly. To that end, solvent water molecules of crystallization contribute to the establishment of extensive hydrogen-bonding interactions throughout the lattice of **1** bestowing to it considerable stability.

4.2. The Ni(II)–quinic acid binary system speciation

A well-defined form of a metal–organic binary species such as **1** requires that an in-depth knowledge of its solution identity and properties is established. To this end, the aqueous solution study on the distribution of species arising in the binary system Ni(II)–quinic acid: (a) aids significantly in the understanding of the nature of various species forming as a function of pH and the stoichiometry of the reagent partners involved, and (b) provides a direct correlation of the physicochemical profile of the proposed species with the structure and properties of the species in the solid state (**1**). In this regard, the species prevailing in the requisite aqueous speciation bear a 1:2 Ni:L stoichiometry. In line with this stoichiometry, mononuclear $[NiL_2]^0$ and $[NiL_2H_{-1}]^-$ species emerge as competent participants in the pH distribution. Beyond that, mononuclear $[Ni(II)]^{2+}$ and $[NiH_{-1}]^+$ species emerge as complementary representative compounds of the aqueous binary distribution in different pH-ranges. Complex $[NiL_2]^0$ dominates in the low to physiological pH range. Its almost constant % fraction of total Ni(II) (30%) in the low and physiological pH range up to pH 8, indicates a preference over other species that could bear quinate ligands. It portrays a species containing a Ni(II) metal ion bearing two quinate ligands and likely two water molecules, thus bestowing an octahedral coordination environment to the central metal ion. In that respect, the $[NiL_2]^0$ species correlates the nature of the proposed solution species with that of **1** in the solid state. That, in turn, implies that compound **1** upon dissolution turns into $[NiL_2]^0$ giving up one quinate ligand. Consequently, **1** is likely not a species existing in solution, but rather one that emerges through favored lattice dynamics upon crystallization from the reaction mixture originally employed. It is worth noting that no 1:1 Ni:L species were proposed through the aqueous solution studies. Collectively, the data of the aqueous speciation relate the existence of the $[NiL_2]^0$ species at pH values around the specific pH value employed for the synthesis of that complex, with **1** ultimately crystallizing out of solution. This thesis is in line with recently isolated complexes of Co(II) with quinic acid at variable pH values in the corresponding binary aqueous speciation [58]. Hence, the idea of (a) synthesizing and isolating the proposed $[NiL_2]^0$ species, and (b) converting the $[NiL_2]^0$ species to **1** upon increasing the quinate:Ni(II) molar ratio (or influencing other factors) in the synthetic reaction mixture, are currently under investigation in our lab.

Moreover, the aqueous speciation studies suggest that other binary species exist at higher pH values (>7.5), including the $[NiL_2H_{-1}]^-$ complex. The composition of that complex presents a synthetic challenge that will shed light into that pH region of the aqueous speciation diagram, pinpointing specific structural features borne by quinate and the bound water molecules to Ni(II). The presence of Ni(II) bearing the same number of quinates at a higher pH as the $[NiL_2]^0$ dominant complex, but with an additional deprotonated aquo ligand (most likely), attests to its significance as a competent partner in the aqueous distribution diagram (albeit at a lower % fraction), explicitly projecting a variable chemical reactivity between Ni(II) and quinate as a function of pH.

4.3. Relevance of Ni(II) aqueous speciation to physiology and/or Ni(II) toxicity

The role of nickel in various structures and compartments in cells has been widely investigated and includes both normal physiological functions as well as toxic effects. As an exogenous inorganic cofactor, Ni(II) has been shown to exhibit physiological and/or aberrant effects (e.g. toxicity) with all the concomitant consequences to the integrity of organisms. As an enzyme metal cofactor and inducer of pathogenic physiologies, Ni(II) could exert influence on biochemical processes in cell structures or intercede in the chemistry of cellular (metal)homeostasis [59] by promoting binary and ternary interactions with cellular organic targets of both low and high molecular mass. Quinic acid is a suitable form of an organic substrate–ligand (a) present in plant fluids and circulating within plant structures, and (b) poised to seek chelation to divalent metal ions, such as Ni(II). In so doing, it establishes a binary Ni(II)–quinic acid system, which in the pH-range of plant physiological functions, generates a distribution of species with distinct physicochemical properties and potential (bio)chemical activity. Metal-linked biochemical activity has been observed in plants, emphasizing the ability of their cells to seek and identify metal ions or organic nutrients (a) essential to maintaining of their physiology [60], and/or (b) competent in combating (phyto)toxicity [61,62] events. To that end, the herein data signify the importance of the form, type and nature of Ni(II)–L (L = hydroxycarboxylate chelator) interactions potentially associated with the maintenance/compromise of cellular physiology or Ni(II) toxicity. In this respect, the well-characterized species **1** relates to the $[NiL_2]$ complex as the dominant species present in the aqueous speciation of the binary Ni(II)–quinic acid system. In plants, the chemistry of Ni(II), represented by well-defined soluble species such as $[NiL_2]^0$, may also reflect critical aspects of its interactive chemistry with other α-hydroxycarboxylic acids.

In humans, on the other hand, aberrant Ni(II) reactivity may influence processes (sister chromatid exchange, signaling pathways, transcription factor chemistry, etc.) linked to various manifestations of Ni(II) toxicity, potentially leading to allergic [63], respiratory and carcinogenic phenotypes [64]. In all of the aforementioned cases, soluble and bioavailable forms of Ni(II) constitute (a) the key to understanding the genetic and epigenetic (bio)chemistry unfolding in cellular compartments, organs and tissues, and (b) targets of ongoing research seeking to comprehend the intricate chemistry of Ni(II) toxicity at the molecular level. In this challenging field, efforts to understand further details of binary and ternary interactions of Ni(II), associated with soluble and bioavailable species currently eluding characterization, are ongoing in our labs.

5. Conclusion

The present endeavor (a) projects the complexity of the Ni(II)–quinic acid solution speciation in aqueous media and the diversity of species expected to arise as a function of pH and molecular Ni(II):quinate stoichiometry, (b) defines the physicochemical properties of a well-defined and characterized Ni(II)–quinate species **1** isolated at a specific pH value and its partner $[NiL_2]^0$ in solution projected through the aqueous speciation studies, and (c) links the pH-dependent bioinorganic chemistry of low molecular mass binary Ni(II)–(O-containing)organic substrate species with further binary and ternary interactions that might promote any potential activity relating to Ni(II) physiology or toxic effects on fundamental structures within cellular fluids.

Acknowledgments

This work was supported by a "Pythagoras" grant from the National Ministry of Education and Religious Affairs, and by a "PENED" grant co-financed by the E.U.-European Social Fund (75%) and the Greek Ministry of Development-GSRT (25%).

Appendix A. Supplementary data

CCDC 644650 contains the supplementary crystallographic data for **1**. These data can be obtained free of charge via http://www.ccdc.cam.ac.uk/conts/retrieving.html, or from the Cambridge Crystallographic Data Centre, 12 Union Road, Cambridge CB2 1EZ, UK; fax: (+44) 1223 336 033; or e-mail: deposit@ccdc.cam.ac.uk. Supplementary data associated with this article can be found, in the online version, at doi:10.1016/j.poly.2008.12.045.

References

[1] E. Denkhaus, K. Salnikow, Crit. Rev. Oncol. Hemat. 42 (2002) 35.
[2] S.O. Moussa, K. Morsi, J. Alloy. Compd. 426 (2006) 136.
[3] A.M. Brennenstuhl, T.S. Gendron, R. Cleland, Corros. Sci. 35 (1993) 699.
[4] G. Winter, T. Buhrke, O. Lenz, A.K. Jones, M. Forgber, B. Friedrich, Fed. Eur. Biochem. Soc. Lett. 579 (2005) 4292.
[5] R.K. Watt, P.W. Ludden, Cell. Mol. Life. Sci. 56 (1999) 604.
[6] E. Haslam, in: Shikimic Acid: Metabolism and Metabolites, Wiley and Sons, New York, 1993.
[7] A.J. Pittard (Ed.), *Escherichia coli* and *Salmonella*: Cellular and Molecular Biology, ASM Press, Washington, DC, 1996.
[8] R. Bentley, Crit. Rev. Biochem. Mol. Biol. 25 (1990) 307.
[9] M. Jezowska-Bojczuk, P. Kaczmarek, W. Bal, K.S. Kasprzak, J. Inorg. Biochem. 98 (2004) 1770.
[10] G. Gran, Acta Chem. Scand. 29 (1950) 559.
[11] G. Gran, Analyst 77 (1952) 661.
[12] F.J.C. Rossotti, H. Rossotti, J. Chem. Educ. 42 (1965) 375.
[13] G. Schwarzenbach, Complexometric Titrations, Interscience, New York, 1960, p. 83.
[14] Micro TT2050 Titrator Quick Guide, Crison Instruments, Alella, Spain, 1985.
[15] H.M. Irving, M.G. Miles, L.D. Petit, Anal. Chim. Acta 38 (1967) 475.
[16] P. Gans, B. O'Sullivan, Talanta 51 (2000) 33.
[17] H.S. Harned, B.B. Owen, The Physical Chemistry of Electrolytic Solutions, 3rd ed., Reinhold Publishing Corp., New York, 1958.
[18] P. Gans, A. Sabatini, A. Vacca, J. Chem. Soc., Dalton Trans. (1985) 1195.
[19] L. Zékány, I. Nagypál, G. Peintler, PSEQUAD for Chemical Equilibria, Technical Software Distributions, Baltimore, 1991.
[20] L. Alderighi, P. Gans, A. Ienco, D. Peters, A. Sabatini, A. Vacca, Coord. Chem. Rev. 184 (1999) 311.
[21] N.V. Plyasunova, Y. Zhang, M. Muhammed, Hydrometallurgy 48 (1998) 43.
[22] B.J. Colston, V.J. Robinson, Analyst 122 (1997) 1451.
[23] SMART-NT, Version 5.0, Brucker AXS, Madison, WI, 1998.
[24] SAINT-NT, Version 5/6.0, Brucker AXS, Madison, WI, 1999.
[25] SHELXTL-NT, Version 5.1, Brucker AXS, Madison, WI, 1998.
[26] Z.H. Zhou, Y.J. Lin, H.B. Zhang, G.D. Lin, K.R. Tsai, J. Coord. Chem. 42 (1997) 131.
[27] E.N. Baker, H.M. Baker, B. Anderson, R.D. Reeves, Inorg. Chim. Acta 78 (1983) 281.
[28] Y. Guo, D. Xiao, E. Wang, Y. Lu, J. Lü, X. Xu, L. Xu, J. Sol, State Chem. 178 (2005) 776.
[29] J. Strouse, S.W. Layten, E. Strouse, J. Am. Chem. Soc. 99 (1977) 562.
[30] M. Menelaou, C.P. Raptopoulou, A. Terzis, V. Tangoulis, A. Salifoglou, Eur. J. Inorg. Chem. (2005) 1957.
[31] R. Swanson, W.H. Ilsley, A.G. Stanislowski, J. Inorg. Biochem. 18 (1983) 187.
[32] R.C. Bott, D.S. Sagatys, D.E. Lynch, G. Smith, C.H.L. Kennard, T.C.W. Mak, Aust. J. Chem. 44 (1991) 1495.
[33] Y. Inomata, T. Haneda, F.S. Howell, J. Inorg. Biochem. 76 (1999) 13.
[34] N. Barba-Behrens, F. Salazar-Garcia, A.M. Bello-Ramirez, E. Garcia-Baez, M.J. Rosales-Hoz, R. Contreras, A. Flores-Parra, Transition Met. Chem. 19 (1994) 575.
[35] I. Bkouche-Walksman, Acta Crystallogr., Sect. C 50 (1994) 62.
[36] G. Hata, Y. Kitano, T. Kaneko, H. Kawai, M. Mutoh, Chem. Pharm. Bull. 40 (1992) 1604.
[37] R. Codd, T.W. Hambley, P.A. Lay, Inorg. Chem. 34 (1995) 877.
[38] A.B.P. Lever, in: Inorganic Electronic Spectroscopy, 2nd ed., Elsevier, Amsterdam, 1984, pp. 507–511.
[39] C. Djordjevic, M. Lee, E. Sinn, Inorg. Chem. 28 (1989) 719.
[40] G.B. Deacon, R.J. Philips, Coord. Chem. Rev. 33 (1980) 227.
[41] M. Matzapetakis, C.P. Raptopoulou, A. Tsohos, B. Papaefthymiou, N. Moon, A. Salifoglou, J. Am. Chem. Soc. 120 (1998) 13266.
[42] M. Matzapetakis, C.P. Raptopoulou, A. Terzis, A. Lakatos, T. Kiss, A. Salifoglou, Inorg. Chem. 38 (1999) 618.
[43] J.J. Borrás-Almenar, J.M. Clemente-Juan, E. Coronado, B.S. Tsukerblat, J. Comput. Chem. 22 (2001) 985.
[44] Program 66, Quantum Chemistry Program Exchange, Indiana University, Bloomington, IN, 1986.
[45] M. Clifford, Tea and Coffee Trade J. 159 (1987) 35.
[46] B. Luethy-Krause, I. Pfenninger, W. Landolt, Trees – Struct. Funct. 4 (1990) 198.
[47] G.V. Bakore, M.S. Bararia, Z. Phys. Chem. (Leipzig) 242 (1969) 102.
[48] Z. Warnke, E. Kwiatkowski, Rocz. Chem. 47 (1973) 467.
[49] B. Mayer, R. Medancic, B. Grabaric, I. Filipovic, Croat. Chem. Acta 51 (1978) 151.
[50] G.H. Thun, W. Guns, F. Verbeek, Anal. Chim. Acta 37 (1967) 332.
[51] T. Matusinovic, I. Filipovic, Croat. Chem. Acta 58 (1985) 227.
[52] M.S. El-Ezaby, N.M. Shuaib, H.M. Marafie, M.M. Hassan, J. Inorg. Biochem. 33 (1988) 161.
[53] J. Lerivrey, B. Dubois, P. Decock, G. Micera, J. Urbanska, H. Kozlowski, Inorg. Chim. Acta 125 (1986) 187.
[54] C. Jubert, A. Mohamadou, C. Gérard, S. Brandes, A. Tabard, J.-P. Barbier, Inorg. Chem. Commun. 6 (2003) 900.
[55] A.A. Mokhir, E. Gumienna-Kontecka, J. Swiatek-Kozlowska, G.E. Petkova, O.I. Fritsky, L. Jerzykiewicz, A.A. Kapshuk, T.Y. Sliva, Inorg. Chim. Acta 329 (2002) 113.
[56] S. Lacour, V. Deluchat, J.-C. Bollinger, B. Serpaud, Talanta 46 (1998) 999–1009.
[57] M. Matzapetakis, N. Karligiano, A. Bino, M. Dakanali, C.P. Raptopoulou, V. Tangoulis, A. Terzis, J. Giapintzakis, A. Salifoglou, Inorg. Chem. 39 (2000) 4044.
[58] M. Menelaou, A. Konstantopai, C. Mateescu, H. Zhao, C. Drouza, N. Lalioti, A. Salifoglou, Inorg. Chem. (2009), submitted for publication.
[59] G.W. Zamponi, E. Bourinet, T.P. Snutch, J. Membrane Biol. 151 (1996) 77.
[60] S.A. Kim, M.L. Guerinot, FEBS Lett. 581 (2007) 2273.
[61] L.P. Weng, A. Wolthoorn, T.M. Lexmond, E.J. Temminghoff, W.H. van Riemsdijk, Environ. Sci. Technol. 38 (2004) 156.
[62] L.P. Weng, T.M. Lexmond, A. Wolthoorn, E.J. Temminghoff, W.H. van Riemsdijk, Environ. Toxicol. Chem. 22 (2003) 2180.
[63] L. Peltonen, Contact Dermatitis 5 (1979) 27.
[64] K.S. Kasprzak, F.W. Sunderman Jr., K. Salnikow, Mutat. Res. 533 (2003) 67.